



Molecular Crystals and Liquid Crystals Science and Technology. Section A. Molecular Crystals and Liquid Crystals

Publication details, including instructions for authors and subscription information:

<http://www.tandfonline.com/loi/gmcl19>

Magnetic Properties of (C₁TEX-TTF)FeBr₄(X=S, Se)

Masaya Enomoto^a, Akira Miyazaki^a & Toshiaki Enoki^a

^a Department of Chemistry, Faculty of Science,
Tokyo Institute of Technology, Ookayama 2-12-1,
Meguro-ku, Tokyo, 152-8551, Japan

Version of record first published: 24 Sep 2006

To cite this article: Masaya Enomoto, Akira Miyazaki & Toshiaki Enoki (1999):
Magnetic Properties of (C₁TEX-TTF)FeBr₄(X=S, Se), Molecular Crystals and Liquid
Crystals Science and Technology. Section A. Molecular Crystals and Liquid Crystals,
335:1, 293-302

To link to this article: <http://dx.doi.org/10.1080/10587259908028873>

PLEASE SCROLL DOWN FOR ARTICLE

Full terms and conditions of use: <http://www.tandfonline.com/page/terms-and-conditions>

This article may be used for research, teaching, and private study purposes.
Any substantial or systematic reproduction, redistribution, reselling, loan,

sub-licensing, systematic supply, or distribution in any form to anyone is expressly forbidden.

The publisher does not give any warranty express or implied or make any representation that the contents will be complete or accurate or up to date. The accuracy of any instructions, formulae, and drug doses should be independently verified with primary sources. The publisher shall not be liable for any loss, actions, claims, proceedings, demand, or costs or damages whatsoever or howsoever caused arising directly or indirectly in connection with or arising out of the use of this material.

Magnetic Properties of (C₁TEX-TTF)FeBr₄(X=S, Se)

MASAYA ENOMOTO, AKIRA MIYAZAKI and TOSHIKI ENOKI

*Department of Chemistry, Faculty of Science, Tokyo Institute of Technology,
Ookayama 2-12-1, Meguro-ku, Tokyo 152-8551, Japan*

The correlation between the magnetic properties and crystal structure of isostructural π -d interaction systems (C₁TEX-TTF)FeBr₄ (X=S, Se) is investigated by crystal structure analysis and magnetic susceptibility measurements. These salts form a sheet structure consisting of one-dimensional anion zigzag chains and donor dimers, the latter of which bridge between two anion chains. The susceptibility, to which only Fe³⁺ ($S=5/2$) spins contribute as a triangle-based spin ladder system, shows antiferromagnetic phase transitions at $T_N=4.2$ K and 3.6K for X=S and Se, respectively. Below T_N , weak ferromagnetism appears due to the Dzyaloshinski-Moriya interaction when the field is applied along one of the spin hard-axes. The difference between the two salts in the weak ferromagnetic transition suggests that the interaction between two Fe³⁺ spin ladders is reduced by a half with changing X=S to Se.

Keywords: π -d interaction; weak ferromagnetism; TTF derivative; spin canting; spin ladder; Dzyaloshinski-Moriya interaction

INTRODUCTION

Organic donor molecules, such as TTF derivatives, form a large variety of charge transfer complexes and radical ion salts by reacting with acceptors or

anions. These planar-shaped TTF derivatives tend to be arranged in a face-to-face and/or side-by-side fashion to form a one- or two-dimensional structure. Consequently, the overlap of the π -electron wave functions between adjacent donors produces a low dimensional extended electronic structure, which is stabilized in a metallic or insulating state depending on the detailed feature of the structure. When we employ some transition metal anions that have localized d -electron spins as the constituents of the complexes, the d -electron spins are expected to interact with the donor π -electrons. The π - d interaction will produce itinerant electron magnetism in the case of metallic π -electron systems or π - d composite magnetism if the π -electron system is in the insulating state^[1,2]. One of the most characteristic properties of organic donor molecules is that they are easy to modify a part of their constituent elements. In addition, the substitution of one anion with another one tends to give isostructural salts when these anions have the same structure. Accordingly, if a salt forms the same structure with changing the components of the donor or the anion, we can directly investigate the substitution effect between the isostructural salts^[3]. Especially, it is known that some types of atom substitution, such as Fe to Ga or S to Se, easily give isostructural salts. As a result, we can control the crystal structure and the magnetic properties of the salts by the atom substitution.

In this study, we investigate the magnetic properties of isostructural π - d composite systems $(C_1\text{TEX-TTF})\text{FeBr}_4$ ($X=\text{S}, \text{Se}$) in relation to the substitutional effect between $X=\text{S}$ and Se . The employment of $C_1\text{TET-TTF}$ (4,5-bis(methylthio)-4',5'-(ethylenedithio)tetrathiafulvalene) and $C_1\text{TESe-TTF}$ (4,5-bis(methylthio)-4',5'-(ethylenediseleno)tetrathiafulvalene) (Fig. 1) as donors is expected to give a multi-channel exchange interaction network, since possible inter-molecular interactions are extended to two different directions, namely, along the short side and long side of the donor molecules. The introduction of an FeBr_4^- 3d electron spin system is expected to provide interesting π -electron-mediated magnetic systems when it is incorporated with the donor network.

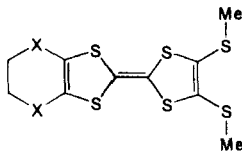


FIGURE 1 The molecular structure of $C_1\text{TEX-TTF}$ ($X=\text{S}, \text{Se}$).

EXPERIMENTAL

C₁TET-TTF^[4,6] and C₁TESe-TTF^[7,8] were prepared according to the previous reports. Single crystals of (C₁TET-TTF)FeBr₄ and (C₁TESe-TTF)FeBr₄ were obtained by a galvanostatic anodic oxidation method under a stationary current of 0.50-2.00 μ A for a synthetic period of 3-4 weeks using 5mg of C₁TEX-TTF, 30-50mg of (*n*-Bu₄N)FeBr₄ as a counter anion and 15cm³ of ethanol as a solvent. In addition, single crystals of isostructural non-magnetic (C₁TET-TTF)GaBr₄ were obtained by using (*n*-Bu₄N)GaBr₄ under the same synthesis condition to that for the FeBr₄⁻ salt. The crystal structures were determined by a single crystal X-ray diffraction method using a Rigaku AFC-7 four-circle diffractometer. The reflection data were collected in the range of $2\theta=5$ to 55 degrees. Their structures were solved with the direct methods using SHELXS-86, then refined with the full-matrix least-squares method using SHELXL-93. The coordinates of hydrogen atoms were calculated geometrically. The magnetic susceptibilities were measured using Quantum-Design MPMS-5 SQUID magnetometer up to a field of 5T in the temperature range 1.8-300K.

EXPERIMENTAL RESULTS

The obtained salts are isostructural with each other with a 1:1 donor/anion composition in monoclinic space group *C2/c*. Fig. 2(a) shows the unit cell of (C₁TET-TTF)FeBr₄. Head-to-tail donor dimers are stacked to form a twisted columnar arrangement along the *c*-axis, where no inter-dimer atomic contacts are shorter than or in the same range to the corresponding van der Waals distances, implying the absence of the inter-dimer interaction along the *c*-axis. The anion molecules form a one dimensional zigzag chain structure extended along the *b*-axis. The ratio of the inter-anion Br-Br distance to the corresponding van der Waals distance (van der Waals ratio) is estimated at 1.02 and 1.05 for (C₁TET-TTF)FeBr₄ and (C₁TESe-TTF)FeBr₄, respectively, suggesting the presence of the inter-anion exchange interaction paths along the *b*-axis. Moreover, there are close contacts between an anion and its neighboring donor dimer on the (10 $\bar{1}$) plane, as evidenced by the fact that the van der Waals ratios of the Br-X distance are 0.99 and 0.96 - 0.97 for X=S and X=Se, respectively. Therefore, we cannot ignore the interaction between adjacent two anion chains, which are bridged by the dimers. As a whole, as

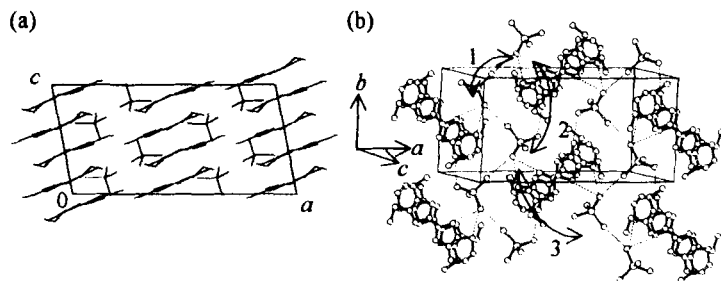


FIGURE 2 Crystal structure of $(C_1\text{TEX-TTF})\text{FeBr}_4$ ($X=\text{S}, \text{Se}$). (a) The unit cell viewed along the b -axis. (b) The projection to the $(10\bar{1})$ plane. The thin solid and dotted lines indicate the short Br-Br and Br-X contacts, respectively. Solid arrows give three super-exchange paths; Fe-Br-Br-Fe (path 1), Fe-Br-D-Br-Fe (path 2), Fe-Br-(D)₂-Br-Fe (path 3), where D denotes a donor molecule.

shown in Fig. 2(b), the structure of these salts is featured by the composite layers composed of anion chains and donor dimers on the $(10\bar{1})$ plane. The inter-anion interaction along the direction perpendicular to the $(10\bar{1})$ plane is negligibly small since the van der Waals ratio of the shortest Br-Br contact is larger than 1.5. This fact suggests that adjoining sheets are independent from each other taking into account the absence of the inter-dimer interaction between the layers.

Figs. 3(a) and (b) show the temperature dependence of the magnetic susceptibility in an applied field of 1 T and the magnetization curve at 2 K for $(C_1\text{TET-TTF})\text{FeBr}_4$, respectively. The susceptibility obeys the Curie-Weiss law in the high temperature range, where the Curie constant C and the Weiss temperature Θ are estimated at $C=4.6 \text{ emu K/mol}$ and $\Theta=-18 \text{ K}$, respectively. The observed Curie constant is explained in terms of only high-spin Fe^{3+} $S=5/2$ spins, hence no contribution of the donor π -electrons to the localized spin system is observed. Therefore, the π -electron spins on the donor molecules are stabilized in the singlet ground state due to the dimerized structure where one hole having a $S\approx 1/2$ is given to a donor according to the 1:1 donor-to-anion ratio. The singlet formation in the donor dimer is supported by the magnetic susceptibility of isostructural $(C_1\text{TET-TTF})\text{GaBr}_4$, which is found to have no localized spins. At low temperatures, the susceptibility shows a short-range order hump around 10 K which is

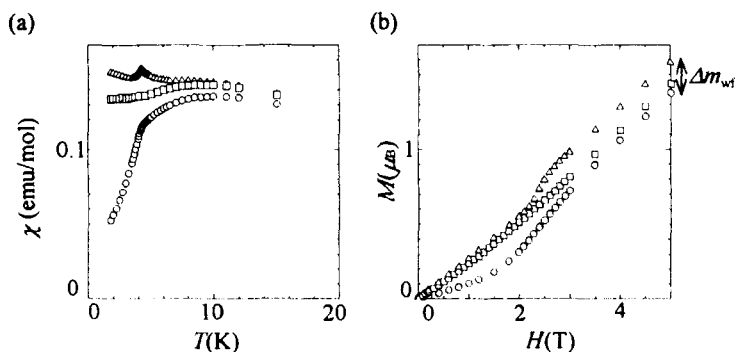


FIGURE 3 The temperature dependence of the susceptibility at $H=1$ T (a) and the magnetization curves at 2 K (b) for (C₁TET-TTF)FeBr₄ (\circ : $H \parallel a$ -axis, \triangle : $H \parallel b$ -axis, \square : $H \parallel c$ -axis). Δm_{wf} denotes the induced magnetization due to the weak ferromagnetism.

accompanied by an antiferromagnetic transition at $T_N \approx 4.2$ K. When the external field is applied parallel to the a -axis, the susceptibility decreases with decreasing temperature below T_N , while, in the field parallel to the b - and c -axes, the susceptibility shows less temperature dependent behavior below T_N . This proves that the spin easy axis is oriented parallel to the a -axis. It should be mentioned that under the field parallel to the b -axis, there is a small cusp at T_N , which is followed by a gradual increase on the low temperature side of T_N . This behavior can be explained by the weak ferromagnetic behavior. The magnetization curve shows a spin-flop transition at $H_{sf} = 2.3$ T when the field is applied parallel to the a -axis, consistent with the result of the susceptibility measurement. As to the c -axis, the magnetization curve shows ordinary hard axis behavior. However, if the field is applied parallel to the b -axis, an additional magnetization appears in the magnetization curve above a transition field of $H_{wf} = 2.3$ T, where the induced magnetization is estimated at $\Delta m_{wf} = 0.21 \mu_B$. Taking into account the feature of the weak ferromagnetism emerging in the susceptibility around T_N in the field $H \parallel b$ -axis, the induced magnetization can be explained in terms of spin canting, where the canting angle is estimated at 4.7° .

Figs. 4(a) and (b) show the temperature dependence of the susceptibility and the magnetization curve for (C₁TESe-TTF)FeBr₄, respectively. The susceptibility associated with Fe³⁺ spins obeys the Curie-Weiss law in the high

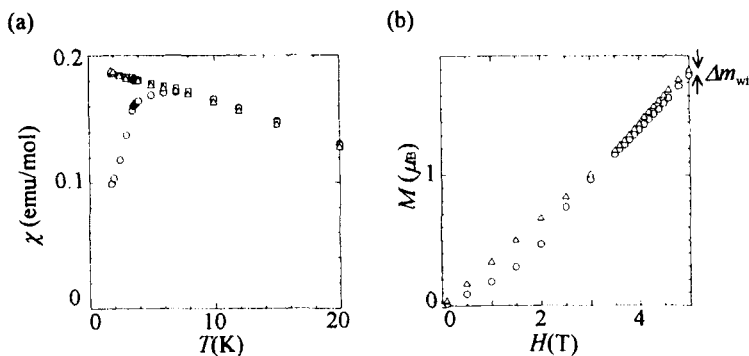


FIGURE 4 The temperature dependence of the susceptibility at $H=1\text{T}$ (a) and the magnetization curves at 2K (b) for $(\text{C}_1\text{TESe-TTF})\text{FeBr}_4$ (\circ : $H \parallel a$ -axis, \triangle : $H \parallel b$ -axis, \square : $H \parallel c$ -axis).

temperature range with $\Theta = -13\text{K}$. Then, it shows a short range order hump around 6K which is sharper than that of $(\text{C}_1\text{TET-TTF})\text{FeBr}_4$. An antiferromagnetic transition takes place at $T_N = 3.6\text{K}$. The measurements of the anisotropy in the susceptibility suggest that the easy axis is oriented parallel to the a -axis similar to that in $\text{X}=\text{S}$. The magnetization curves of $(\text{C}_1\text{TESe-TTF})\text{FeBr}_4$ have the similar trend with the same spin axis dependence to those of $\text{X}=\text{S}$. Namely, a spin-flop transition takes place at $H_{\text{sf}} = 2.3\text{T}$, while a weak ferromagnetic transition occurs at $H_{\text{wf}} = 4.0\text{T}$ where the induced magnetization is estimated at $\Delta m_{\text{wf}} = 0.04\mu_B$, giving a spin canting angle of 0.9° .

DISCUSSION

Firstly, we discuss the magnetic structures of the two salts based on the information on the crystal structures and magnetic properties. As can be seen in Fig. 2, the structural consideration suggests that the magnetic interaction network is composed of three-kinds of super-exchange interactions; that is, the $\text{Fe-Br}\cdots\text{Br-Fe}$ path (path 1) along the anion one-dimensional zigzag chain, the $\text{Fe-Br}\cdots\text{D}\cdots\text{Br-Fe}$ (D: donor molecule) path (path 2) along one anion chain which bypasses every two FeBr_4^- anions and the $\text{Fe-Br}\cdots(\text{D})_2\cdots\text{Br-Fe}$ path (path 3) where a donor dimer bridges between adjoining anion chains. From the consideration on the strengths of the interaction, the topological feature of the interaction network is characterized. The combination of J_1 and J_2 in one

anion chain gives triangle-based ladder structure. Moreover, J_3 contributes to the inter-ladder interaction. In general, the strength of the exchange interaction depends on the numbers of atoms, which participate in its super-exchange paths. Namely, it increases as the number increases. Therefore, the strengths of the exchange interactions are considered to be on the order of $J_1 > J_2 > J_3$. Here, we discuss the magnetic structure of the ladder system on the basis of the molecular field scheme with J_1 and J_2 , where the neglect of the weakest interaction J_3 is justified according to the later discussion. Assuming that the structure of the individual ladder is characterized with the two sublattice system as exhibited in Fig. 5, the relation between Θ and T_N is given by the following equations,

$$\Theta = \frac{N(g\mu_B)^2 S(S+1)}{6k} \cdot \frac{1}{2} (A + \Gamma) \quad (1)$$

$$-\frac{\Theta}{T_N} = \frac{A + \Gamma}{A - \Gamma}, \quad (2)$$

$$A = \frac{2z_1 J_1}{N/2 \cdot (g\mu_B)^2}, \quad \Gamma = \frac{2z_2 J_2}{N/2 \cdot (g\mu_B)^2}, \quad (3)$$

where $z_1=2$ and $z_2=2$ are the numbers of the neighboring spins connected by J_1 and J_2 , respectively. N is the number of the spin sites in a ladder. For the estimation of J_1 and J_2 , we employ the value of the short-range order hump temperature as the representative of T_N , because the discussion is based on the molecular field frame and the rather small difference between T_N and the temperature of the hump proves the validity of the discussion at least in the temperature range above the temperature of the hump. Using the value of $-\Theta/T_N=1.8$ for X=S and 2.2 for X=Se, we obtain $J_1 \sim 1.20\text{K}$, $J_2 \sim 0.35\text{K}$ and $J_1 \sim 0.81\text{K}$, $J_2 \sim 0.31\text{K}$ for X=S and Se, respectively. The second nearest exchange interaction J_2 that bridges every two spin sites causes spin frustration effect, resulting in the reduction in the value of T_N compared with the value of Θ . The finding that J_2/J_1 is larger in X=Se than in X=S proves that (C₁TESe-TTF)FeBr₄ is affected more seriously by the spin frustration. The increase in J_2/J_1 in X=Se is consistent with the fact that the van der Waals ratio of the Br-Br distance for J_1 is extended by the substitution of S with Se, whereas that of the Br-X distance for J_2 is shortened.

The magnetization curves also give information on the exchange interactions in relation to the spin-flop transition and the saturation field as

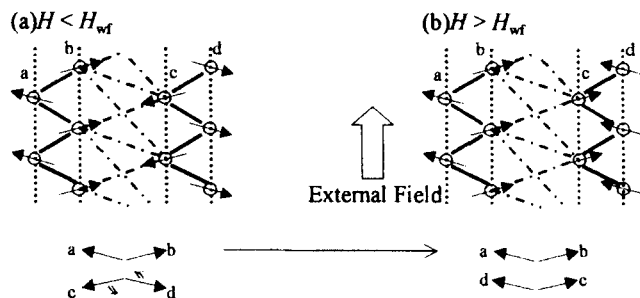


FIGURE 5 Four-sublattice magnetic structure model (a) above and (b) below the weak ferromagnetic transition field H_{wf} . Sublattices are denoted by a, b, c and d. The solid, dotted and dot-dashed lines give J_1 , J_2 and J_3 , respectively.

expressed by, $H_{sf} = \sqrt{H_A(2H_E - H_A)}$ and $H_C = 2H_E - H_A$, where H_A , H_E and H_C are the exchange field, the anisotropy field and the saturation field of the magnetization, respectively. The saturation field is estimated as a field at which the extrapolated line of the linearly increasing hard axis magnetization curve to the high field range reaches the saturation magnetization $M_s = Ng\mu_B S = 5.1\mu_B$ ($S=5/2$). The experimental observation gives $H_C=18\text{T}$, $H_{sf}=2.3\text{T}$ for $X=\text{S}$ and $H_C=15\text{T}$, $H_{sf}=2.3\text{T}$ for $X=\text{Se}$. Consequently, we obtain $H_A=0.29\text{T}$ and 0.35T , $H_E=9.2\text{T}$ and 7.7T for $X=\text{S}$ and Se , respectively. H_E is related to A and Γ as,

$$H_E = AM - \Gamma M, \quad M = N/2 \cdot g\mu_B \langle S \rangle. \quad (4)$$

From the above equations, we obtain $J_1 \sim 1.76\text{K}$, $J_2 \sim 0.51\text{K}$ and $J_1 \sim 1.68\text{K}$, $J_2 \sim 0.64\text{K}$ for $X=\text{S}$ and Se , respectively. The obtained values are in semi-quantitative agreement with those estimated from Eq. (1).

Next, we discuss the weak ferromagnetism. The experimental finding suggests that the additional contribution to the magnetization appears above a transition field of H_{wf} . This means that the spontaneous magnetizations Δm_{wf} related to the weak ferromagnetism are cancelled between the sublattices below H_{wf} . In order to explain the origin of the weak ferromagnetism, we employ a four-sublattice model with a canted spin configuration as given in Fig. 5 where J_3 connects adjacent ladders. Figs. 5(a) and (b) show the possible spin arrangements for $H < H_{wf}$ and $H > H_{wf}$ which explain all of the

experimental results self-consistently. In this model, we take the *a*- and *b*-axes as the spin easy axis and the direction of the spontaneous magnetization of weak ferromagnetism, respectively. The absence of an inversion center between two adjacent FeBr₄⁻ anions suggests the Dzyaloshinski-Moriya interaction^[9,10] as the origin of the spin canting. The energies of the spin system below and above H_{wf} are expressed in terms of J_1 , J_2 and J_3 in the following equations,

$$E_i = -2J_1SS + 2J_2SS - 3J_3SS. \quad (H < H_{\text{wf}}) \quad (5)$$

$$E_i = -2J_1SS + 2J_2SS + 3J_3SS. \quad (H > H_{\text{wf}}) \quad (6)$$

where the numbers of the neighboring spins are given to be $z_1=2$, $z_2=2$ and $z_3=3$ for J_1 , J_2 and J_3 , respectively. Therefore, the difference between the energies,

$$E_f - E_i = 6J_3SS, \quad (7)$$

is equated to the energy gain produced by the weak ferromagnetic transition as given by

$$E_f - E_i = \Delta m_{\text{wf}} H_{\text{wf}}. \quad (8)$$

Using the values obtained by the experiments, $H_{\text{wf}} = 2.3\text{ T}$, $\Delta m_{\text{wf}} = 0.21\mu_B$ for (C₁TET-TTF)FeBr₄ and $H_{\text{wf}} = 4.0\text{ T}$, $\Delta m_{\text{wf}} = 0.06\mu_B$ for (C₁TESe-TTF)FeBr₄, the estimation gives $J_3 = 9 \times 10^{-3}$ and $4 \times 10^{-3}\text{ K}$ for X=S and Se, respectively, which is two orders of magnitude smaller than J_2 . This suggests the validity of the spin-ladder model for the present systems. It should be noted that the strength of J_3 is two times larger in X=S than Se. The emphasized importance of J_3 in X=S can be explained by the S/Se substitution-induced structural modification, that is, the intra-dimer transfer integral, which contributes to a part of the super-exchange path 3, is about 3% larger in X=S than X=Se.

Finally, we comment on another evidence for the two-dimensionality of the present magnetic systems. From the specific heat, 42% of the total magnetic spin entropy is consumed below T_N in (C₁TET-TTF)FeBr₄^[11]. The theoretical values of consumed magnetic entropy below T_N are given to be 29% and 76% for the two- and three-dimensional Ising models, respectively. Comparing the experimental value with the theoretical values, we conclude that this salt has two-dimensional magnetic structure, consistent with the experimental findings in the present work.

SUMMARY

Isostructural cation radical salts (C₁TEX-TTF)FeBr₄ (X=S, Se) are investigated as π -electron-mediated molecular magnet systems. The exchange network is characterized to be a triangle-based spin ladder system associated with Fe³⁺ $S=5/2$ spins, where the donor- π -electron-mediated super-exchange paths play an important role in their magnetically ordered structures. Under the field, weak ferromagnetism appears, which is explained in terms of spin-canting configurations brought about by the Dzyaloshinski-Moriya interaction.

Acknowledgements

The authors would like to express their sincere thank to Prof. H. Tanaka for fruitful discussion. This work was supported in part by a Grant-in-Aid for Scientific Research on Priority Areas (No. 10149101 "Metal-assembled Complexes") from Ministry of Education, Science, Sports and Culture, Japan. M. E. was supported by Inoue Foundation for Science.

References

- [1] T. Enoki, M. Enomoto, M. Enomoto, K. Yamaguchi, N. Yoneyama, J. Yamaura, A. Miyazaki and G. Saito, *Mol. Cryst. Liq. Cryst.*, **285**, 19 (1996).
- [2] T. Enoki, J. Yamaura, and A. Miyazaki, *Bull. Chem. Soc. Jpn.*, **70**, 2005 (1997).
- [3] A. Miyazaki, M. Enomoto, M. Enomoto, T. Enoki and G. Saito, *Mol. Cryst. Liq. Cryst.*, **305**, 425 (1997).
- [4] G. Steimecke, H-J. Sieler, R. Kirmse and E. Hoyer, *Phosphorus and Sulfur*, **7**, 49 (1979).
- [5] K.S. Varma, A. Bury, N.J. Harris and A.E. Underhill, *Synthesis Commun.*, 837 (1987).
- [6] A. Ootsuka, *private communication*.
- [7] L.R. Melby, H.D. Hartzler and W.A. Sheppard, *J. Org. Chem.*, **39**, 2456 (1974).
- [8] R-M. Olk, A. Rohr, B. Olk and E. Hoyer, *Z. Chem.*, **28**, 304 (1988).
- [9] I. Dzyaloshinsky, *J. Phys. Chem. Solid*, **4** 241 (1958).
- [10] T. Moriya, *Phys. Rev. Letters*, **4** 228 (1960).
- [11] M. Enomoto, A. Miyazaki and T. Enoki, *private communication*.